

# Inhibition Mechanism of Oxalhydrazide on Reinforcing Steel in Pore Solution Contaminated by 3.5%NaCl - Experimental and Theoretical Study

Smrithy Subash<sup>1\*</sup>, Sumedha Moharana<sup>1</sup>, and Yamini Sudha Sistla<sup>2</sup>

<sup>1</sup>Shiv Nadar University, Department of Civil Engineering, Uttar Pradesh 201314, India

<sup>2</sup>Shiv Nadar University, Department of Chemical Engineering, Uttar Pradesh 201314, India

**Abstract.** Concrete is one among the most consumed materials on the planet secondary to water. However, the degradation of concrete happens due to the corrosion of reinforcement. Although the pore solution of concrete is alkaline, the corrosion of rebars in concrete is triggered due to aggressive ions like chlorides entering the concrete. The most common method of corrosion inhibition is by utilising corrosion inhibitors which when added to the concrete stays in the pore solution and prevents the corrosion of surface of rebars from aggressive ions. Although there are number of inhibitors, the rise in corrosion deterioration demands the need for new potential inhibitors which are highly effective in different aggressive environments. This study is based on the corrosion of rebars in simulated concrete pore solution in the presence of 3.5% NaCl with oxalhydrazide as the potential inhibiting material. The corrosion behaviour of rebar is obtained by electrochemical studies using EIS and potentiodynamic polarization and theoretically analysed employing molecular mechanics and molecular dynamics simulations. The experimental results revealed that the inhibitor is effective in reducing the corrosion and the values of binding energy of the inhibitors on rebar surface also go well with the experimental results. Oxalhydrazide is found effective in minimizing the attack of chloride ion on rebar in pore solution.

## 1 Introduction

Concrete is the second most consumed material on the planet with an annual consumption of 3 tonnes per person globally[1]. Premature deterioration of reinforcing steel possesses a great threat to the future existence of concrete structures. Concrete acts as an electrolyte with steel embedded and the ionic composition which is alkaline is called pore solution whose substitute can be simulated based on the chemical composition[2]. The simulated concrete pore solution is being used for corrosion studies due to the complex nature of reinforced concrete system[3,4]. The steel corrosion results in losses which affects the economy of the country. Therefore, the corrosion of mild steel has been extensively studied. There are many types of inhibitors employed for the protection of steel including both inorganic and organic/green inhibitors[5] which is obtained from natural sources. They form a layer over the steel substrate and protect them from corrosion.

The incorporation of organic inhibitors is an efficient and cost reduction technique of combating the corrosion on steel[6,7] compared to inorganic ones. These organic inhibitors functions effectively by the process of adsorption onto the surface of steel[6,8,9]. Considerable number of studies based on the organic corrosion inhibitors have been done to find an effective and efficient corrosion inhibitor to mitigate steel

corrosion[6,8–16]. The heteroatoms such as O, N, S and P[17] and its presence in the inhibiting molecules is found to improve the corrosion inhibiting property of the inhibitor as well as the physical and chemical adsorption of these inhibiting molecules on the metal surface[18]. These inhibitors contain lone pair of electrons which fills the vacant d orbitals of metal atoms either by sharing or backdonation, hence effective on getting adsorbed onto the metal surface. Therefore organic inhibitors forms a layer over the surface of metal and protects from the corroding ions[19]. As the inhibition performance of the heteroatoms follows the order  $P > S > N > O$ [20] there has been an extensive research carried out on the investigation of inhibitors containing these elements. Hydrazides are one such compound having both N and O elements. The behaviour of oxalhydrazide (OHD) otherwise called ethanedihydrazide has already been investigated on mild steel[13]. But previous studies have not reported the utilization of OHD on the rebar in pore solution.

Therefore, this work mainly aims to investigate the corrosion inhibition property of oxalhydrazide inhibitor on the reinforced steels in pore solution with 3.5% NaCl corroding solution. The study inculcates a detailed investigation both experimentally – using the electrochemical measurements such as Electrochemical Impedance Spectroscopy (EIS), polarization measurements and computationally – by employing Density Functional Theory (DFT) and Molecular Dynamics (MD) based calculations [6,8,11,14,21]. It is due to the fast, simple and cheap features, molecular

\* Corresponding author: [ss831@snu.edu.in](mailto:ss831@snu.edu.in)

dynamics simulation based on COMPASS forcefield is being widely preferred by researchers for adsorption studies[6,22]. Molecular Dynamics (MD) simulation based technique is based on the laws in classical physics, where the Newtons equations of motions are used to determine the position of atomic particles[12,23]. MD simulations facilitates in exploring the adsorption behaviour of inhibitors in different electrolytic media[6]. From the previous report[13] this inhibitor shows a maximum efficiency at 0.5mM concentration, so this concentration is chosen for this study. The experimental results based on electrochemical impedance and potentiodynamic polarization studies were supported using molecular simulations based on binding energy calculations.

## 2 Materials and experimental methods

### 2.1 Materials

#### 2.1.1 Preparation of Steel sample

The samples of reinforcing steel employed for the study were Thermo Mechanically Treated (TMT) bars of Fe415 grade. The effect of blank corrodant was studied on a rebar specimen having dimension 12mm diameter and 5cm long with an exposed surface area of 20 cm<sup>2</sup>. The preparation of sample surface was done according to ASTM G-01. The rebars were initially washed with 10v/v% HCl acid solutions for 5 minutes to remove black oxide and then cleaned with distilled water[24]. The samples were then ground with SiC grit paper starting with 200 -1500 mesh followed by washing in distilled water, degreased in acetone and cleaned in ethanol. The surface prepared samples are soldered at one end to facilitate electrical connection for electrochemical testing and covered with epoxy on that face to prevent the damage to the connection. The curved surface area and bottom round face of the 5cm long rebar section was exposed to the pore solution with and without inhibitor in the presence of 3.5% NaCl blank corrodent.

#### 2.1.2 Alkaline Pore Solution-Inhibited and Uninhibited

The simulated pore solution which substitutes the concrete pore solution was prepared by mixing 8.33g of NaOH, 3.36g KOH and 2.64g of Ca(OH)<sub>2</sub> in 1000ml distilled water which is mixed using magnetic stirrer for 24 hours and filtered using whatmann filter paper[24]. This solution was then supplied with 3.5% NaCl to make the blank corrodent. The pH of the solution was found to be alkaline around 12.5 at 25°C. This solution is taken as the uninhibited solution for the study.

The inhibited pore solution was prepared by adding a 0.5mM[13] stock solution of Oxalhydrazide (OHD) - a non-toxic inhibiting chemical and mild irritant to eyes and skin upon direct contact, shown in **Fig. 1** into the pore solution containing NaCl corrodent. The 0.1181g of OHD in 100ml formaldehyde is used for the preparation of 100ml stock solution. 5ml of stock

solution is added to 95 ml pore solution with NaCl for the preparation of 100ml 0.5mM inhibited solution.

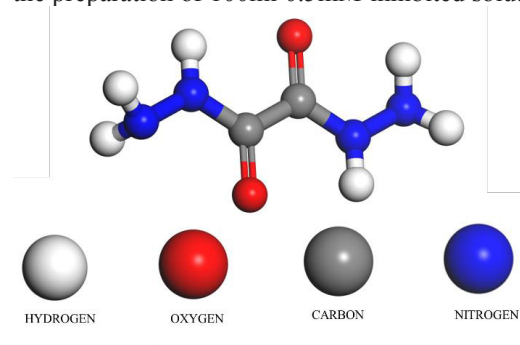


**Fig. 1.** Molecular Structure of oxalhydrazide

### 2.2 Methodology

#### 2.2.1 Electrochemical measurements

A Biologic (SP 300 computer controlled) operated by the EC-Lab<sup>®</sup> software is used to perform the electrochemical experiments and the results were fitted using EC-Lab<sup>®</sup>. All the electrochemical studies employed the use of three-electrode setup. The rebar steel sample, Ag/AgCl and platinum coil as the working (WE), reference (RE) and counter (CE) electrode respectively were employed for the study as shown in **Fig. 2**. Initially the working electrode was subjected to Open Circuit Potential (OCP) measurement for which the setup needs to be kept in an undisturbed phase for nearly 10 minutes until the system reaches a steady state potential.

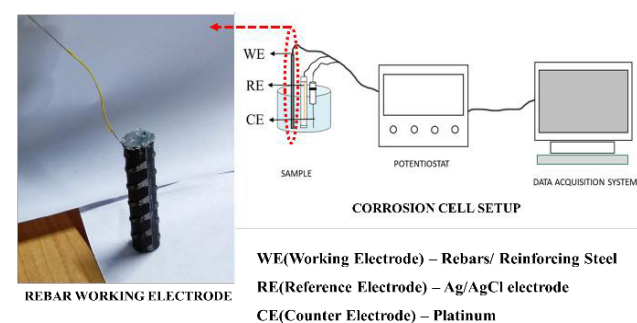


**Fig. 2.** Corrosion Cell and Rebar Working Electrode

The rebar samples were kept 1 hour prior to the electrochemical measurements in solutions with and without inhibitor. The potentiodynamic polarisation studies involve application of potentials between -0.2V to +0.2V at a scanning rate of about 1mV/s. The extrapolation of linear segments of Tafel curve was done to obtain the corrosion current ( $i_{corr}$ ) density, corrosion potential ( $E_{corr}$ ) and cathodic and anodic slopes of Tafel curve ( $\beta_a$  and  $\beta_c$  respectively)[25].

The impedance spectroscopy using electrochemical techniques (EIS) were conducted between a range of 100kHz to 100mHz frequency at an amplitude of  $\pm 5$  mV AC peak-to-peak. The appropriate equivalent circuit is chosen for fitting the impedance data to obtain the necessary parameters to analyse the spectra including the charge transfer resistance ( $R_{ct}$ ).

### 2.2.2 Quantum Chemistry and Molecular Dynamics Studies

The molecular simulations were performed using Biovia Material Studio by Dassault system software version 2022. The effect of electronic properties and structural parameters on adsorption mechanism and inhibition efficiency of inhibitor molecules on metallic iron (Fe) surface were investigated using quantum chemical calculations. The inhibition efficiency of various inhibitor molecules was analysed with the help of reactivity parameters [11] such as, the energy of highest occupied molecular orbital ( $E_{\text{HOMO}}$ ), energy of lowest unoccupied molecular orbital ( $E_{\text{LUMO}}$ ), the HOMO-LUMO energy gap [26,27] reflecting the reactivity of the molecule, hardness and softness, electronegativity ( $\chi$ ) and the fraction of transferred electrons from the inhibitor to Fe surface ( $\Delta N$ ), are investigated in the present study[28].

Initially, using molecular builder, the structure of the inhibitor was built. The optimization of the molecular structure was carried out using Dmol3 module with Generalized Gradient Approximation (GGA) functional Perdew-Burke-Ernzerhof (PBE) and DNP basis set [29]. The geometry optimized structure was verified for the absence of frequencies of negative vibrations to make sure that the structure has stable configuration on the potential energy surface. The Fe (110) surface was built from Fe unit cell. A vacuum slab model of Fe (110) was constructed by applying periodic boundary condition on 'X' and 'Y' directions and a 20 Å vacuum applied in the 'Z' direction. The structure was then optimized using CASTEP module of Material Studio. The optimization was done by GGA functional PBE. In order to understand the energetically most stable orientation of a single inhibitor molecule with respect to the Fe surface, the molecule was kept close to the Fe (110) surface in three different orientations. The three orientations are (i) vertical (OHD1), (ii) horizontal (OHD2) and (iii) aligned to the Fe surface (OHD3). The geometry of « inhibitor + Fe(110) » was then optimized for the three orientations. The binding energy ( $E_{\text{binding}}$ ) of the inhibitor molecule with Fe (110) surface for each orientation was calculated using equation 1[5].

$$E_{\text{binding}} = E_{\text{total}} - (E_{\text{surface}} + E_{\text{inhibitor}}) \quad (1)$$

Where,

$E_{\text{total}}$  is the electronic energy of the structure comprising of the « inhibitor molecule + Fe(110) surface »,  $E_{\text{surface}}$  indicates the electronic energy of metallic surface Fe(110), and  $E_{\text{inhibitor}}$  implies the energy of the single inhibitor molecule.

The molecular dynamic (MD) simulations using Forcite module was performed to understand the interaction of corroding solution comprising of 500 water molecules and 5  $\text{Na}^+$  (violet colour) and 5  $\text{Cl}^-$  (green colour) molecules with the inhibitor molecule attached Fe (110) surface. For all the simulations, COMPASS III forcefield was used. The electrostatic interactions were represented using Ewald summation method while van der Waals interactions were

represented using atom based method with a cut off distance of 15 Å. The binding energy of the corroding solution with the inhibitor attached Fe surface was obtained using equation 2[30]. The binding energy corresponding to the corroding solution in the absence of inhibitor molecule was obtained using equation 3.

$$E_{\text{binding}} = E_{\text{total}} - (E_{\text{surface+inhibitor}} + E_{\text{solution}}) \quad (2)$$

Where,

$E_{\text{total}}$  is the energy of configuration comprising of « metal surface + inhibitor + NaCl solution »,  $E_{\text{surface+inhibitor}}$  is the energy of « inhibitor molecule + metallic surface Fe (110) », and  $E_{\text{solution}}$  indicates the energy of NaCl corroding solution.

$$E_{\text{binding}} = E_{\text{total}} - (E_{\text{surface}} + E_{\text{solution}}) \quad (3)$$

Where,

$E_{\text{total}}$  corresponds to the energy of the system comprising of both Fe (110) surface and solution,  $E_{\text{surface}}$  indicates the energy of metallic surface Fe (110), and  $E_{\text{solution}}$  is the energy of the corroding solution comprising of  $\text{Na}^+$ ,  $\text{Cl}^-$  and  $\text{H}_2\text{O}$  molecules.

### 2.2.3 Simulation of surface, solution, and inhibitor molecule

The body centered cubic (BCC) bulk crystal structure of iron (Fe) was imported from the database of Material studio. According to the reported literature, Fe (110) surface is more energetically stable in comparison to other planes and therefore it can have effective adsorption sites[23]. The Fe bulk crystal was cleaved for (110) miller plane to construct Fe (110) surface. A supercell was built by expanding the surface in X and Y directions with Fe (110) slab thickness of 20 Å. A vacuum cell was built by increasing the length in Z-direction in order to accommodate the inhibitor and water molecules. During geometry optimization, the atoms in bottom layers were constrained at their own bulk positions to resemble the bulk substrate whereas the atoms of upper layer were allowed to fully relax[6].

In general, inhibitor molecules tend to reduce the adsorption strength of corrosive solutions such as NaCl on metal surfaces. The concentration and type of inhibitor molecules have great influence on the interaction strength of corrosive molecules on metal surface. The corrosive solution that we considered in the present study is aqueous solution of sodium chloride (NaCl). For preparing the corrosive solution (mentioned as solution) medium,  $\text{H}_2\text{O}$ ,  $\text{Cl}^-$ ,  $\text{Na}^+$  molecules were built using molecule builder. The structures were geometry optimized using Dmol3 using GGA functional PBE and DNP basis set. Electrostatic potential based partial charges were applied to each atom. The solvent medium was then constructed with 500 molecules of  $\text{H}_2\text{O}$ , 5 molecules each of  $\text{Cl}^-$  and  $\text{Na}^+$  ions. The number of molecules represent 1M solution of NaCl. With the help of layer builder, a layered model of solvent, inhibitor and the Fe(110) slab was constructed to generate the model for "surface+inhibitor+solution". The geometry optimization was done after layer construction with

Forcite module using “smart” algorithm and a forcefield of COMPASS III was employed. The obtained optimized geometry was studied under microcanonical ensemble (NVE) equilibration run for 300 ps at 298 K and 1 atm. Further, the system was simulated using canonical (NVT) ensemble for 500 ps of equilibration runs using random initial velocities followed by production simulations for 250 ps. Nose-Hoover-Langevin thermostat was employed for temperature controlled NVT runs. The energy of this system was considered as  $E_{total}$ . A similar run was performed to get the energy of “surface+inhibitor” model as  $E_{surface+inhibitor}$  and solution the energy of NaCl solution as  $E_{solution}$  using the same MD simulation protocol for calculating  $E_{total}$ .

### 3 Results and discussion

#### 3.1 Experimental Results

##### 3.1.1 Electrochemical Impedance Results (EIS)

EIS is a widely used non-destructive method employed to understand the kinetics and mechanisms of electrochemical system. The Nyquist plot representing the impedance values of rebar samples in inhibited and uninhibited solutions for an hour is shown in **Fig. 3**. The equivalent circuit best found to fit the impedance data is given as inset in **Fig. 3**. The  $R_1$  is the solution resistance,  $R_2$  and  $Q_2$  are the resistance and capacitance offered by the passive film in alkaline pore solution,  $R_3$  and  $Q_3$  indicates the charge transfer resistance and the double layer capacitance offered at the interface of steel rebar and electrolyte respectively[31]. The ideal capacitance was replaced by a constant phase element to best resemble the inhomogeneity of the surface due to surface roughness[32,33]. The circuit fitted curves were represented in continuous green lines in **Fig. 3**, and the values obtained after fit was given in **Table 1**.

The solution resistance of inhibited solution was found to be more than that of uninhibited due to the reduction of conductivity of the inhibited solution with inhibitor molecules.

**Table 1** Fitted values of EIS of rebar in pore solution with and without inhibitor in 3.5% NaCl

Type of solution	Inhibited	Uninhibited
$R_1$ ( $\Omega$ )	2.156	1.904
$Q_2$ ( $Fs^{(a-1)}$ )	0.065	0.544
$a_2$	0.397	0.54
$R_2$ ( $\Omega$ )	9590	209.1
$Q_3$ ( $Fs^{(a-1)}$ )	0.083	0.003
$a_3$	0.382	0.540
$R_3$ ( $\Omega$ )	307.4	3.69

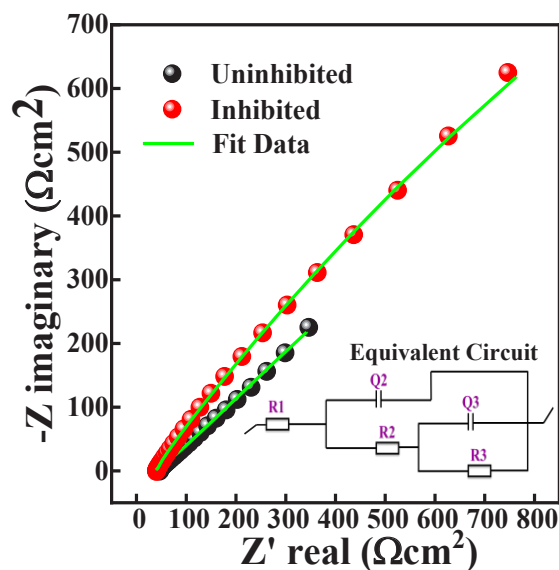


**Fig. 3.** Complex plane plot and inset shows Equivalent Circuit used for fitting.

The increase in film capacitance of the passivation layer of the uninhibited solution was mainly attributed either due to the thinning of passive layer formed or due to the increased porosity of the surface mainly because of the pitting caused by the chloride ions. This shows that the film capacitance of passive layer increases with the reduced film thickness of the surface hence the variation in film capacitance may be an indication of pitting of steel surface. This indicates the evolution of passivation layer of OHD molecules, which remains intact on rebar surface in pore solution in the presence of NaCl ions. The resistance offered by passivation layer is very high in inhibited solution when compared with the resistance of the passive film offered by uninhibited solution. But the absence of inhibitors causes the breakdown of these passivation layer and ultimately due to the attack from aggressive chloride ions there are chances of occurrence of pitting on the steel surface which is clear in uninhibited solutions[34]. Whereas the charge transfer resistance values in both inhibited and uninhibited cases is reduced when compared with the passive film resistance due to the depassivation of the passive film on the working electrode due to exposure to chloride ions for more time[35]. But the charge transfer resistance value of inhibited rebar sample was found to be higher than uninhibited.

##### 3.1.2 Tafel Polarization

In order to authenticate the result obtained from EIS, the potentiodynamic tests were conducted on rebar samples in pore solution contaminated by 3.5% NaCl in the presence and absence of OHD inhibiting molecules and the results were presented[36] in **Table 2**.

The corrosion current density,  $I_{corr}$  for uninhibited case is found to be around  $194.744 \mu A/cm^2$  which is found to be 23.89 times higher than the inhibited solution. The higher corrosion rate,  $R_{corr}$  in the absence of inhibitor is mainly due to the spontaneous and harsh attack of the NaCl molecules onto the steel surface

making the surface dissolvable and vulnerable to further attack.

Also, the inhibitor molecules adsorbed on the steel surface is high as it is evident from the formation of passivation layer even for small exposure time of 1 hour. Therefore, with the presence of inhibitor and its concentration the anodic and cathodic corrosion currents decreased which ultimately reduced the corrosion current and corrosion rates. Therefore, the results from tafel polarization exhibited in **Fig. 4** shows similar trend as in case of EIS values. Based on  $I_{corr}$  the inhibition efficiency of the OHD is found to be around 95.81% in pore solution which seems to take part significantly in mitigating corrosion.

**Table 2** Electrochemical parameters obtained after fitting tafel polarization data

Type of solution	Inhibited	Uninhibited
$E_{corr}$ (mV)	-616.998	-590.382
$I_{corr}$ ( $\mu$ A/cm <sup>2</sup> )	8.149	194.744
$\beta_c$ (mV)	36.300	125.0
$\beta_a$ (mV)	103.200	8.580
$R_{corr}$ (mm/year)	0.096	2.293

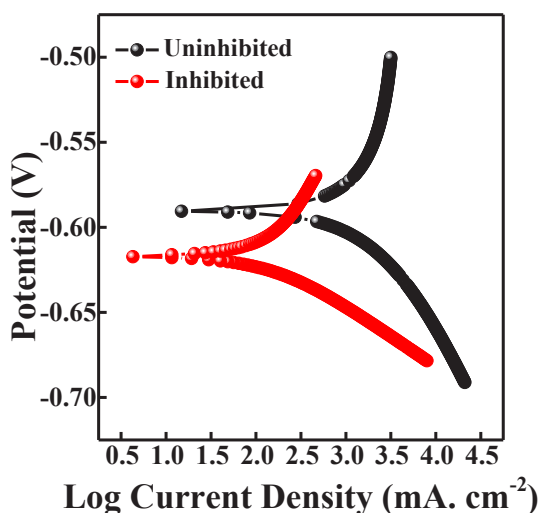


**Fig. 4.** Tafel polarization data of steel rebar with and without inhibitor in pore solution in 3.5% NaCl

### 3.2 Simulation Results

#### 3.2.1 Quantum chemical parameters

The energy of the frontier molecular orbitals  $E_{HOMO}$ ,  $E_{LUMO}$  and the energy gap  $\Delta E$  are significant parameters which represent the reactivity of the organic molecules. The electron donation ability of inhibitor molecule defines the inhibition efficiency. It is therefore concluded that higher  $E_{HOMO}$  causes increased electron donation chances by organic inhibitors onto Fe surface[37] and lower  $E_{LUMO}$  favours increased acceptance of electrons by the organic molecule of

inhibitor from d-orbitals of metal through backdonation. Similarly, the energy gap  $\Delta E = (E_{LUMO} - E_{HOMO})$  of the inhibiting molecule is another indice whose higher value favours lesser reactivity and vice versa[12,38]. Hence the reactivity of the molecule is found to be high due to low  $\Delta E$  therefore its easier for the molecule to donate its electrons.

HOMO and LUMO electron densities of « oxalhydrazide » molecule are as presented in the **Fig. 5**. The values of  $E_{HOMO}$  and  $E_{LUMO}$  suggests that inhibitor has the potential to both accept and donate electrons to the d-orbitals of metal under favourable conditions. The energy gap is the measure of kinetic stability of the inhibitor and a large gap is an indication of charge transfer within the molecule. The molecule having large gap exhibits higher stability and vice versa[10].

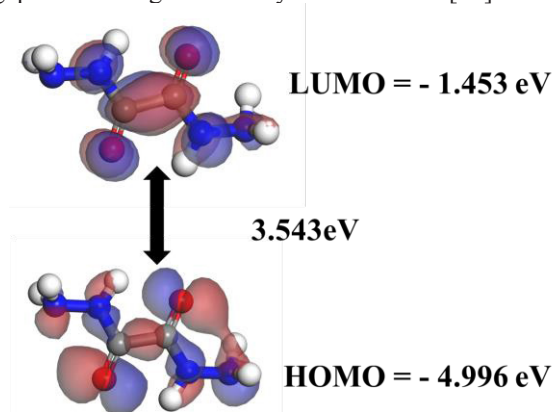


**Fig. 5.** HOMO and LUMO orbitals and the energy gap of “Oxalhydrazide” molecule

The molecule having high stability is supposed to be less reactive chemically. Thus, chemical reactivity is found to be high for soft molecules than hard ones. Thus HOMO - LUMO gap is a clear indication of activity of the organic molecule. Larger gap therefore causes less polarization of molecule resulting in hard molecule with increased stability and lower chemical reactivity. Various reactivity descriptors of oxalhydrazide molecule are given in **Table 3**. The softness value of Oxalhydrazide (OHD) indicates the reason for ease of adsorption on Fe (110) surface enhancing inhibiting effect. The lower electronegativity( $\chi$ ) value explains the tendency to release loosely bounded electrons effortlessly which increases the adsorption of the molecule and indirectly favours the inhibition. The  $\Delta N$  indicating fraction of electron transferred from inhibitor molecule to metallic atom is also given in **Table 3**. If the  $\Delta N$  has a values less than 3.6 ( $\Delta N < 3.6$ ) then the inhibitor molecules are effective in donating electrons thus resulting into the adsorption onto the metallic surface[39].

#### 3.2.2 Calculation of binding energy

The geometry of inhibitor molecule, OHD and the Fe (110) structure were optimised using the module CASTEP in the DFT framework. The orbital cutoff quality was set to fine. The Vanderbilt ultrasoft

pseudopotential[40] was used [41,42] to increase the speed and accuracy[43] of calculations governing the interaction of electron-ion. The structure optimization was based on Broyden–Fletcher–Goldfarb–Shanno (BFGS) algorithm[44]. A 1 x 1 x 1 k-points set was used. The geometric structure of the OHD was optimized in 12 x 12 x 12 Å lattice cell with periodic boundary conditions. To understand the most stable orientation of OHD molecule for adsorption on Fe surface, the binding energy (BE) of OHD on Fe surface was calculated as per the equation 1 for three different orientation and tabulated in **Table 4**. OHD1, OHD2 and OHD3 in **Table 4** is represented in three orientations as shown in **Fig. 6**.

**Table 3** Reactivity descriptors of Oxalhydrazide

Parameter	Equation	Values
$E_{HOMO}$ (eV)	-	-4.996
$E_{LUMO}$ (eV)	-	-1.453
Gap Energy ( $\Delta E$ ) (eV)	$E_{LUMO} - E_{HOMO}$	3.543
Chemical Hardness ( $\eta$ )	$(E_{LUMO} - E_{HOMO})/2$	-1.772
Softness ( $\sigma$ )	$1/\eta$	-0.564
Ionization Potential (IP) (eV)	$-E_{HOMO}$	4.996
Electron Affinity (EA) (eV)	$-E_{LUMO}$	1.453
Electronegativity ( $\chi$ )	$(IP+EA)/2$	3.225
Transferred Fraction of Electrons ( $\Delta N$ )	$(\chi_{Fe} - \chi_{inh})/[2*(\eta_{Fe} - \eta_{inh})]$ $\chi_{Fe} = 4.82\text{eV}, \eta_{Fe} = 0$	0.450

**Table 4** Binding energy calculation for three different orientations of OHD molecule on Fe(110) surface

Types	OHD 1	OHD 2	OHD 3
$E_{Total}$ (eV)	-85357.672	-85357.732	-85358.604
$E_{Surface}$ (eV)	-82988.38	-82988.38	-82988.38
$E_{Inhibitor}$ (eV)	-2361.814	-2361.814	-2361.814
$E_{Binding}$ (eV)	-7.477	-7.537	-8.41
$E_{Binding}$ (kJ/mol)	-721.488	-727.282	-811.444

The highest negative value of BE indicates the highest adsorption strength and energetically stable configuration of « inhibitor + Fe surface ». Higher the adsorption strength, higher will be the inhibition

efficiency. As per **Table 4**, binding energy is observed to be maximum negative for « OHD 3 ». In the OHD 3 orientation, the inhibitor molecule is attached to the Fe surface with almost five binding points which makes the adsorption on the Fe surface strongest among the three orientations studied. The presence of more number of active sites in the structure of inhibiting molecules can result in multisite adsorption and cause excellent geometric blocking[45].

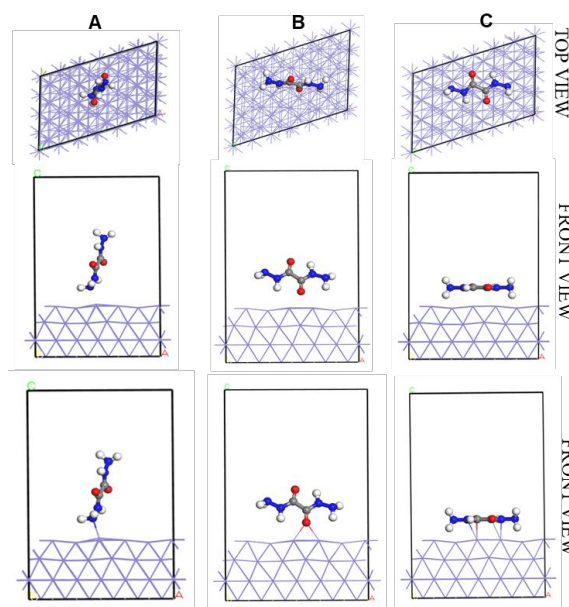


**Fig. 6.** Interaction between OHD and Fe(110) surface in different orientations a) vertical b) horizontal c) aligned parallel to the surface.

The inhibitor's OHD 3 orientation which has highest adsorption with Fe surface was again optimized in the presence of chloride ion (green colour) using same simulation settings and the binding energy of chloride ion are presented in **Table 5** and in **Fig. 7**.

**Table 5** Effect of inhibitor (OHD) on the binding energy of chloride (Cl<sup>-</sup>) ion on Fe(110) surface

Types	OHD 3 + Cl <sup>-</sup>	Types	Fe + Cl <sup>-</sup>
$E_{Total}$ (eV)	-85767.625	$E_{Total}$ (eV)	-83399.159
$E_{Fe SURF+INH}$ (eV)	-85358.604	$E_{Fe SURF}$ (eV)	-82988.38
$E_{Cl^-}$ (eV)	-426.06	$E_{Cl^-}$ (eV)	-426.06
$E_{BINDING}$ (eV)	17.039	$E_{BINDING}$ (eV)	15.281
$E_{BINDING}$ (kJ/mol)	1644.106	$E_{BINDING}$ (kJ/mol)	1474.423

In the **Table 5**, the column «OHD 3 + Cl<sup>-</sup>» represent the calculations for the binding energy of Cl<sup>-</sup> ion in the presence of the inhibitor OHD where 3 represents the orientation number as per **Table 4** and **Fig. 6**. The column «Fe + Cl<sup>-</sup>» represent the calculations for binding energy of Cl<sup>-</sup> ion in the absence of the inhibitor OHD. The values of binding energy calculated as per equation 1, of chloride ion on Fe surface with and without the inhibitor showed positive values. Positive

binding energy indicates weak interaction. Higher the positive value, weaker the interaction. The higher positive binding energy is observed in the presence of inhibitor. This indicates that the energy needed for the chloride ion to bind to the Fe surface in the presence of OHD inhibitor is more than the energy needed for the chloride ion to bind to the Fe surface in the absence of inhibitor molecule. Therefore, it can be clearly understood that the presence of inhibitor is effective in reducing the adsorption of chloride ion onto the Fe surface.

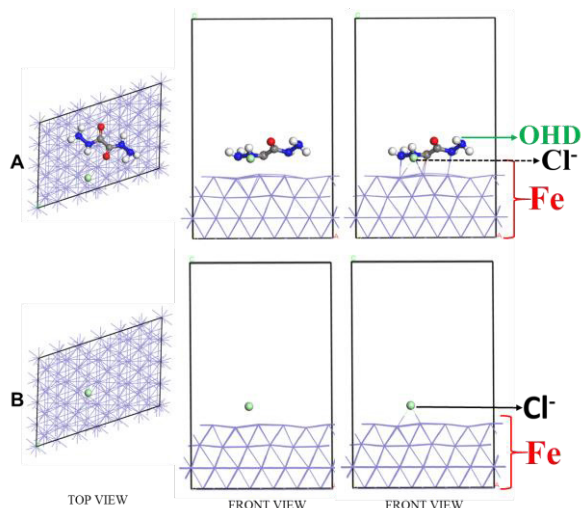


**Fig. 7.** Adsorption of a)  $\text{Cl}^-$  ion on Fe (110) in the presence of inhibitor b)  $\text{Cl}^-$  ion on Fe (110) in the absence of inhibitor

### 3.2.3 Molecular dynamics simulation

The adsorption of inhibitor (OHD) molecule onto the surface of iron was also studied using MD simulations. The binding energy (BE) was computed using equation 1. All the simulations were run using Forcite module of Material Studio. In order to mimic the coating of corrosion inhibitor on Fe surface, adsorption of a layer of 36 OHD molecules was studied. The BE of single OHD molecule was compared with the BE of 36 OHD molecules as reported in **Table 6**.

**Table 6** Binding energy values of single OHD and a layer of 36 OHD molecules on Fe surface using molecular simulation.

Types	OHD	OHD-36
$E_{\text{TOTAL}}$ (kcal/mol)	90.207	5496.419
$E_{\text{INH}}$ (kcal/mol)	177.089	5734.694
$E_{\text{SURF}}$ (kcal/mol)	183.367	183.367
$E_{\text{BINDING}}$ (kcal/mol)	-270.249	-421.642
$E_{\text{BINDING}}$ (kJ/mol)	-1130.721	-1764.15

The optimized structures using classical simulation methods are subjected to dynamics run initially in microcanonical (NVE) ensemble followed by canonical (NVT) ensemble at a temperature of 298 K and pressure of 1 atm. The obtained BE values are presented in **Table**

**6** and the molecular structures used for the simulation are shown in **Fig. 8.**, **Fig. 9.**, **Fig. 10.**

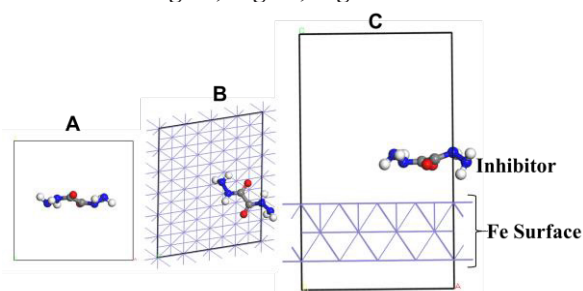


**Fig. 8.** Molecular dynamics simulation of OHD on Fe surface a) OHD molecule b) top view c) front view.

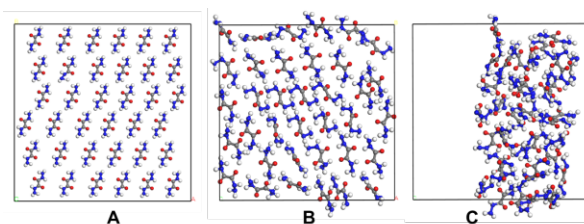


**Fig. 9.** a) 36 OHD molecules before optimization b) geometry optimized 36 OHD molecules c) molecular arrangement of the 36 OHD molecules after dynamics run

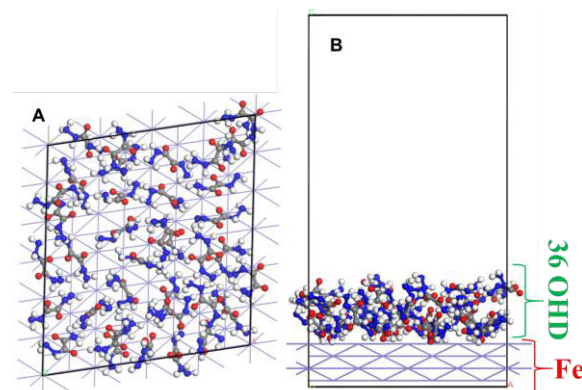


**Fig. 10.** Molecular dynamic simulation of 36 OHD molecules on Fe (110) surface a) top view b) front view

In the **Table 6**, the column OHD refers to the BE for single inhibitor molecule on the Fe (110) substrate and the column OHD-36 refers to the BE of the 36 inhibitor molecules obtained with the help of molecular dynamics simulation [14–16]. The binding energy of single and 36 molecules of OHD adsorption on the Fe surface are -1130.72 kJ/mol and -1764.15 kJ/mol respectively. This indicates strong adsorption of the OHD molecules on Fe(110) surface. The BE of corrosive solution (NaCl) with Fe(110) surface was also studied in the presence of one OHD molecule, 36 OHD molecules and in the absence of inhibitor using MD simulations. The corresponding molecular structures are presented in the **Fig. 11.**, **Fig. 12.**, **Fig. 13.**, respectively. The BE values of corrosive NaCl solution with the Fe surface in the presence of inhibitor molecule (OHD), are compared with the BE in the absence of inhibitor as reported in the **Table 7**.

The results in the **Table 7** clearly indicate that the inhibitor molecule reduces the adsorption energy of the

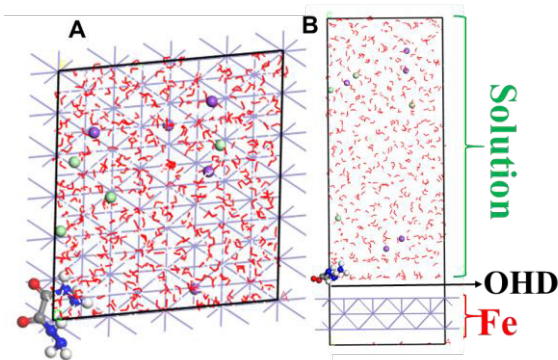


**Fig. 11.** Molecular dynamic simulation of NaCl solution in the presence of single inhibitor on Fe (110) surface a) top view b) front view

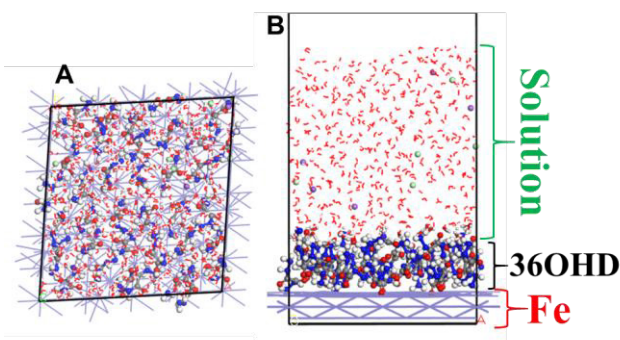


**Fig. 12.** Molecular dynamics simulation of NaCl solution in the presence of a layer of 36 inhibitor molecules on Fe (110) surface a) topview b) frontview

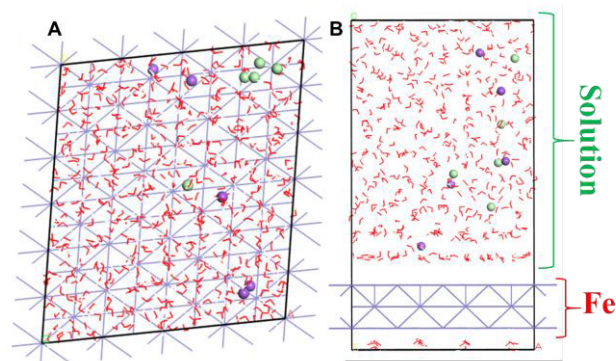


**Fig. 13.** Molecular dynamics simulation of NaCl solution in the absence of inhibitor molecule on Fe (110) surface a) topview b) front view

**Table 7** Binding Energy of NaCl solution with Fe(110) surface and the effect of OHD inhibitor

Types	With Inhibitor		Without inhibitor
	OHD	36OHD	Fe+solution
$E_{TOTAL}$ (kcal/mol)	-6106.95	-1747.737	-13188.02
$E_{SURF+INH}$ (kcal/mol)	90.207	3641.588	183.367
$E_{SOLN}$ (kcal/mol)	-3675.637	-3675.637	-3675.637
$E_{BINDING}$ (kcal/mol)	-2521.52	-1713.69	-9695.75
$E_{BINDING}$ (kJ/mol)	-10550.04	-7170.079	-40567.018

corrosive NaCl solution on Fe surface which can be understood from the less negative values of BE in the presence of OHD and more negative value of BE in the absence of OHD[45] as reported in **Table 7**. Also the BE of NaCl solution on Fe(110) surface in the presence of 36 molecules of OHD is less in comparison to the BE of NaCl in the presence of single OHD which shows that the increased number of inhibitor molecules offers better protection to Fe surface from corroding solution.

#### 4 Conclusion

This study clearly demonstrates the interaction of aggressive NaCl ions in simulated pore solution on the Fe surface and the corrosion inhibiting behaviour of oxalhydrazide (OHD). Results indicate that the OHD has high inhibition efficiency based on the corrosion current density values. The results of EIS go well with potentiodynamic polarization results. The EIS values suggest the presence of two RC loops in the equivalent circuit with the uninhibited case showing reduced thickness of passive films or surface heterogeneity due to pitting caused by chloride ions. The adsorption of molecules of inhibitor on the metal surface seems significant even for small period of exposure. Chlorides at the steel/solution interface gets adsorbed on the steel surface leading to local pitting corrosion damage of the reinforcement in uninhibited case. The experimental results were clearly backed by the simulation results. The binding energy of single OHD inhibitor and 36 molecules of OHD infer chemisorption of OHD molecules on Fe (110) surface. The HOMO LUMO studies and their energy gap clearly indicates that the inhibitor molecules have the tendency to donate and accept electrons from metal d-orbitals. The binding energy of inhibitor placed parallel to the Fe(110) surface is found to be most favourable configuration of interaction having five binding points between OHD and Fe (110) surface. The chloride ions adsorption onto Fe surface was strictly prevented by the presence of OHD inhibitor which was evident from the binding energy of both cases. The binding energy of corroding NaCl solution in the presence and absence of OHD was studied using molecular simulations. The results indicate that the OHD molecules significantly reduce the binding of corroding solution to the Fe surface. Overall, the inhibitor is found very effective in mitigating the corrosion on the surface of rebar in pore solution.

#### Reference

1. C. R. Gagg, Eng. Fail. Anal. **40**, 114 (2014)
2. M. G. Alexander, H. Beushausen, and M. B. Otieno, Dep. Civ. Eng. Univ. Cape T. Concr. Mater. Struct. Integr. Res. Unit 4 (2012)
3. A. H. Yasir, A. S. Khalaf, and M. N. Khalaf, Open J. Org. Polym. Mater. **07**, 1 (2017)
4. H. Bensabra and N. Azzouz, Metall. Mater. Trans. A **44**, 5703 (2013)
5. J. Fu, H. Zang, Y. Wang, S. Li, T. Chen, and X.

6. Liu, *Ind. Eng. Chem. Res.* **51**, 6377 (2012)
7. L. Guo, I. B. Obot, X. Zheng, X. Shen, Y. Qiang, S. Kaya, and C. Kaya, *Appl. Surf. Sci.* **406**, 301 (2017)
8. A. Nid-Bella, B. El Ibrahim, L. Bammou, M. Belkhaouda, M. Aboulhassan, and R. Salghi, *J. Mol. Struct.* **1274**, 134453 (2023)
9. J. Zhang, G. Qiao, S. Hu, Y. Yan, Z. Ren, and L. Yu, *Corros. Sci.* **53**, 147 (2011)
10. A. Kokalj, *Faraday Discuss.* **180**, 415 (2015)
11. K. Rajalakshmi, S. Gunasekaran, and S. Kumaresan, *Indian J. Phys.* **88**, 733 (2014)
12. M. K. Awad, *Can. J. Chem.* **91**, 283 (2013)
13. E. E. Ebenso, C. Verma, L. O. Olasunkanmi, E. D. Akpan, D. K. Verma, H. Lgaz, L. Guo, S. Kaya, and M. A. Quraishi, *Phys. Chem. Chem. Phys.* **23**, 19987 (2021)
14. A. H. Ahmed, E. S. M. Sherif, H. S. Abdo, and E. S. Gad, *ACS Omega* **6**, 14525 (2021)
15. M. V. Diamanti, E. A. Pérez Rosales, G. Raffaini, F. Ganazzoli, A. Brenna, M. Pedferri, and M. Ormellese, *Corros. Sci.* **100**, 231 (2015)
16. M. V. Diamanti, M. Ormellese, E. A. Pérez-Rosales, M. P. Pedferri, G. Raffaini, and F. Ganazzoli, *Nanotechnol. 2010 Adv. Mater. CNTs, Part. Film. Compos. - Tech. Proc. 2010 NSTI Nanotechnol. Conf. Expo, NSTI-Nanotech 2010* **1**, 689 (2010)
17. G. Raffaini, M. Catauro, F. Ganazzoli, F. Bolzoni, and M. Ormellese, *Macromol. Symp.* **404**, 1 (2022)
18. M. El Faydy, F. Benhiba, A. Berisha, Y. Kerroum, C. Jama, B. Lakhrissi, A. Guenbour, I. Warad, and A. Zarrouk, *J. Mol. Liq.* **317**, 113973 (2020)
19. D. K. Verma, Y. Dewangan, A. K. Dewangan, and A. Asatker, *J. Bio- Tribo-Corrosion* **7**, (2021)
20. F. Khan, C. Verma, R. Susai, and M. A. Quraishi, *Eur. Chem. Bull.* **6**, 21 (2017)
21. N. C. Subramanyam, B. S. Sheshadri, and S. M. Mayanna, *Corros. Sci.* **34**, 563 (1993)
22. Ha-Won Song and Velu Saraswathy, *Int. J. Electrochem. Sci.* **2**, 1 (2007)
23. A. Motta, M.-P. Gaigeot, and D. Costa, *J. Phys. Chem. C* **116**, 12514 (2012)
24. H. J. C. Berendsen, in (1999), pp. 3–36
25. S. Mandal, J. K. Singh, D.-E. Lee, and T. Park, *Molecules* **25**, 3785 (2020)
26. H. U. Nwankwo, L. O. Olasunkanmi, and E. E. Ebenso, *Sci. Rep.* **7**, 1 (2017)
27. M. A. Bedair, *J. Mol. Liq.* **219**, 128 (2016)
28. M. K. Awad, M. R. Mustafa, and M. M. A. Elnga, *J. Mol. Struct. Theochem* **959**, 66 (2010)
29. A. Zarrouk, B. Hammouti, A. Dafali, M. Bouachrine, H. Zarrok, S. Boukhris, and S. S. Al-Deyab, *J. Saudi Chem. Soc.* **18**, 450 (2014)
30. M. Ramezanzadeh, Z. Sanaei, G. Bahlakeh, and B. Ramezanzadeh, *J. Mol. Liq.* **256**, 67 (2018)
31. C. Verma, L. O. Olasunkanmi, I. B. Obot, E. E. Ebenso, and M. A. Quraishi, *RSC Adv.* **6**, 15639 (2016)
32. R.-Q. Hou, R.-G. Du, C.-J. Lin, and J.-S. Pan, *J. Electroanal. Chem.* **688**, 275 (2013)
33. J. A. Bardwell and M. C. H. McKubre, *Electrochim. Acta* **36**, 647 (1991)
34. B. Cox and Y.-M. Wong, *J. Nucl. Mater.* **218**, 324 (1995)
35. M. Mobin, I. Ahmad, M. Basik, M. Murmu, and P. Banerjee, *Sustain. Chem. Pharm.* **18**, 100337 (2020)
36. M. Alahiane, R. Oukhrib, Y. A. Albrimi, H. A. Oualid, H. Bourzi, R. A. Akbour, A. Assabbane, A. Nahlé, and M. Hamdani, *RSC Adv.* **10**, 41137 (2020)
37. G. Vengatesh and M. Sundaravadivelu, *J. Adhes. Sci. Technol.* **34**, 2075 (2020)
38. K. F. Khaled and M. A. Amin, *J. Appl. Electrochem.* **38**, 1609 (2008)
39. F. Bentiss, M. Traisnel, H. Vezin, H. F. Hildebrand, and M. Lagrenée, *Corros. Sci.* **46**, 2781 (2004)
40. S. K. Saha and P. Banerjee, *Mater. Chem. Front.* **2**, 1674 (2018)
41. D. Vanderbilt, *Phys. Rev. B* **41**, 7892 (1990)
42. Y. Wang, W. Wang, K.-N. Fan, and J. Deng, *Surf. Sci.* **490**, 125 (2001)
43. A. Kruglikov, A. Vasilchenko, A. Kasprzhitskii, and G. Lazorenko, *RSC Adv.* **9**, 39505 (2019)
44. K. F. Garrity, J. W. Bennett, K. M. Rabe, and D. Vanderbilt, *Comput. Mater. Sci.* **81**, 446 (2014)
45. B. G. Pfrommer, M. Côté, S. G. Louie, and M. L. Cohen, *J. Comput. Phys.* **131**, 233 (1997)
46. L. O. Olasunkanmi, I. B. Obot, M. M. Kabanda, and E. E. Ebenso, *J. Phys. Chem. C* **119**, 16004 (2015)